JOURNAL OF MATERIALS SCIENCE 22 (1987) 251–256

Optical properties of tin in the 2.5 to 40 μm region

S. MAHMOUD
Physics Department, National Research Centre, Cairo, United Arab Republic

The optical constants n and k of evaporated tin deposited on different substrates (potassium bromide and mica-sheet discs) were determined in the 2.5 to 40 μm region by measuring its transmittance. From these values a second step was carried out to determine other physical parameters of tin films. These were the density of conduction electrons, N, the effective collision frequency of the electrons, ν_0, the plasma frequency, ω_0, the velocity on the Fermi surface, V_0, the effective area of the Fermi surface, A_{eff}, and the absorption coefficient, A. The energy-loss functions for surface and volume plasmons show sharp peak at 7.69 μm. These values are compared with those found in earlier work.

1. Survey of previous optical data

The optical constants of a metal are functions of the influence of an electromagnetic wave on the behaviour of the electrons within the metal. It would thus seem that if the optical constants of thin films are different from the constants of the bulk metal, and if they vary with the thickness of the film, it is because the structures of the bulk metal and the films of various thicknesses are all different [1, 2].

The optical constants of metals depend strongly on the conduction electron density as well as on the interaction of electrons with phonons. Golovashkin and Motulevich [3, 4] carried out a simultaneous study of the optical, electrical and several other properties of white tin, evaporated in a vacuum on to a glass substrate. The optical constants of tin were measured at temperatures of 4.2, 78 and 293 K in the wavelength range 0.9 to 12 μm [5]. Therefore, the results were analysed using the method employed earlier [3, 4]. In this analysis, the wavelength range 3 to 12 μm was used and the internal photoeffect contribution to the optical constants could then be neglected. The temperature dependence of the electron–phonon collision frequency was determined as in the case of high-energy light quanta [5].

The optical constants of tin at room temperature have been determined by Motulevich and Shubin [6], as well as by Hodgson [7]. The results reported by Motulevich and Shubin refer only to the spectral range 1.3 to 6.3 μm, in which they agree well with the results of the work of Golovashkin and Motulevich [3, 4]. Hodgson [7] gave his results only in the form of a graph of the dependences of $\log(k^2 - n^2 + 1)$ and $\log(nk/\lambda)$ on $\log \lambda$.

Near-normal incidence reflectance data on vacuum-evaporated white tin films, produced *in situ*, are presented for incident photon energies from 2.1 to 4.5 eV. In addition, the real part of the refractive index has been measured from 14.5 to 20.5 eV by the critical-angle method. Separation of the dielectric constants into contributions due to free and bound electrons indicates interband transitions at 1.2 ± 0.1 and 24.5 ± 0.1 eV, and a further interband transition at approximately 3 eV. Then the energy-loss functions for surface and volume plasmons show sharp peaks at 9.2 and 13.4 eV, respectively, in agreement with electron-energy-loss measurements [8]. Comins [9] has measured the optical constants of liquid tin by an ellipsometric method at wavelengths, mainly in the infrared region, of up to 8 μm and at temperatures up to 1200° C.

The optical properties of globular tin films on Al_2O_3 substrates have been analysed [10]. These films are composed of tin particles with sizes of the order of the wavelength of visible light, and are of interest because of their solar-selective properties. The experimental data show interference film properties at long wavelengths, and a large diffracted component at short wavelengths superimposed on a Lambertian angular distribution. Finally, the optical properties of thin tin films were studied in the infrared region. The mean free path and the specular parameter were determined from the correlation of the electrical and optical results [11].

2. Experimental techniques

Tin films were obtained by evaporating tin of 99.99% purity from a molybdenum boat on to two different substrates (freshly cleaved surface of mica and KBr discs) at room temperature. A pressure of 10^{-4} Pa was maintained in the apparatus. The optical constants of these films were determined from the transmission curves over the spectral range 2.5 to 40 μm using a recording double beam spectrophotometer (Beckman IR 4220) which gives transmission data accurate to within 1%. The radiation from the source travels in two similar paths. One beam passes through the specimen cell, the other through the reference cell. The reference samples are KBr and mica-sheet discs, depending on whether the specimen film of tin is deposited on KBr or mica discs, respectively. The thickness of all these layers was measured by an interference method [12].

0022–2461/87 $03.00 + .12

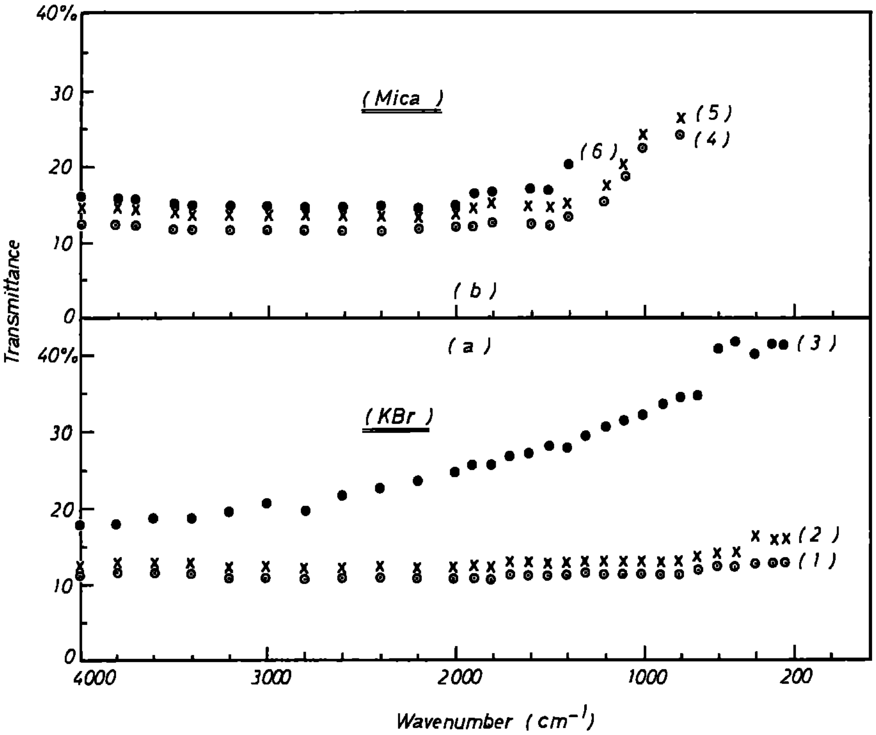

Figure 1 Relations between transmittance and wavenumber (a) on KBr disc, (1) t = 150 nm; (2) t = 130 nm; (3) t = 90 nm; (b) on mica substrate, (4) t = 120 nm; (5) t = 110 nm; (6) t = 100 nm.

3. Results and discussion

It is well known that with specified values of temperature and wavelength the optical constants of a thin film of given thickness are functions of a certain number of factors, the type of support and the temperature of the support at the instant of evaporation; the speed with which the film has been prepared; the degree of vacuum in which the evaporation took place; the type of preparation used and the nature of the residual gas. On the other hand, under well-defined conditions of evaporation the optical constants have been found to vary with the thickness of the film, the temperature and the wavelength of the radiation used in the determination of the constants [1].

It is well known that the structure and defect density of thin vacuum-deposited film depend on the nucleation and growth processes, and the parameters that are important in the study of the latter are sticking coefficient, nucleation density and surface mobility of the adatoms. Considering the coalescence state of the post-nucleation growth of films, as defects are mainly incorporated in the film at this stage, it was found that an increase in the agglomeration of the film and a consequent decrease in the defect density is caused by a decrease in nucleation density and sticking coefficient and an increase in the surface mobility [13, 14]. The surface mobility of the adatoms on the substrate surface is a function of the deposition rate which is constant in the present work, so the sticking coefficient and the nucleation density are the only parameters affecting the defect density and they are dependent on the substrate-deposition pair. Hence, the defect density of tin films deposited on mica differs from that of films deposited on glass [13, 14].

For a thick absorbing film, the transmittance of a film of index $n - ik$ and thickness t is given by [15, 16]

$$T = \frac{16 n_0 (n^2 + k^2)\, e^{-4\pi k t/\lambda}}{[(n + 1)^2 + k^2][(n_0 + n)^2 + k^2]} \quad n > n_0 \qquad (1)$$

where n_0 is the refractive index of the substrate. The extinction coefficient k can be determined at any wavelength from the slope of the curve of ln transmission against thickness for that wavelength according to the equation [15, 16]

$$k = \frac{\lambda}{4\pi}\left(\ln\frac{1}{T_1} - \ln\frac{1}{T_2}\right)\Big/(t_1 - t_2) \qquad (2)$$

The variation of the transmittance, T, of thin films of different thicknesses deposited on to two different substrates (KBr and mica-sheet discs) with variation in wave number (cm^{-1}) is shown in Fig. 1. The transmittance increases gradually as the wavelength increases; moreover, the transmittance decreases on increasing the film thickness and for thickness $\approx$ 150 nm the film becomes opaque in the case of KBr disc and 120 nm in the case of mica substrates. This difference may be attributed to the substrate effect. Earlier measurements of the infra-red transmission of metal films have shown that the transmission increased with increasing wavelength. This phenomenon has been noted by other workers [17].

The spectral behaviour of the real (n), and imaginary (k) parts of the refractive index of tin films could be estimated from Equations 1 and 2. Fig. 2 shows the variation of n and k with wavelength for tin films deposited on KBr discs and mica substrates, respectively.

The electronic theory of metals leads to the following expression [18] for the real dielectric constant (Re ε),

$$\begin{aligned} Re\,\varepsilon &= \varepsilon_0 - \frac{4\pi N e^2}{m(\omega^2 + \nu_0^2)} \\ &\simeq \varepsilon_0 - \frac{\omega_0^2}{(\omega^2 + \nu_0^2)} \qquad (3) \end{aligned}$$

where N is the concentration of the conduction electrons (cm^{-3}), $e = 4.8 \times 10^{-10}$ c.g.s. units is the electronic charge, $m^* = 1.26$ m for tin [19],

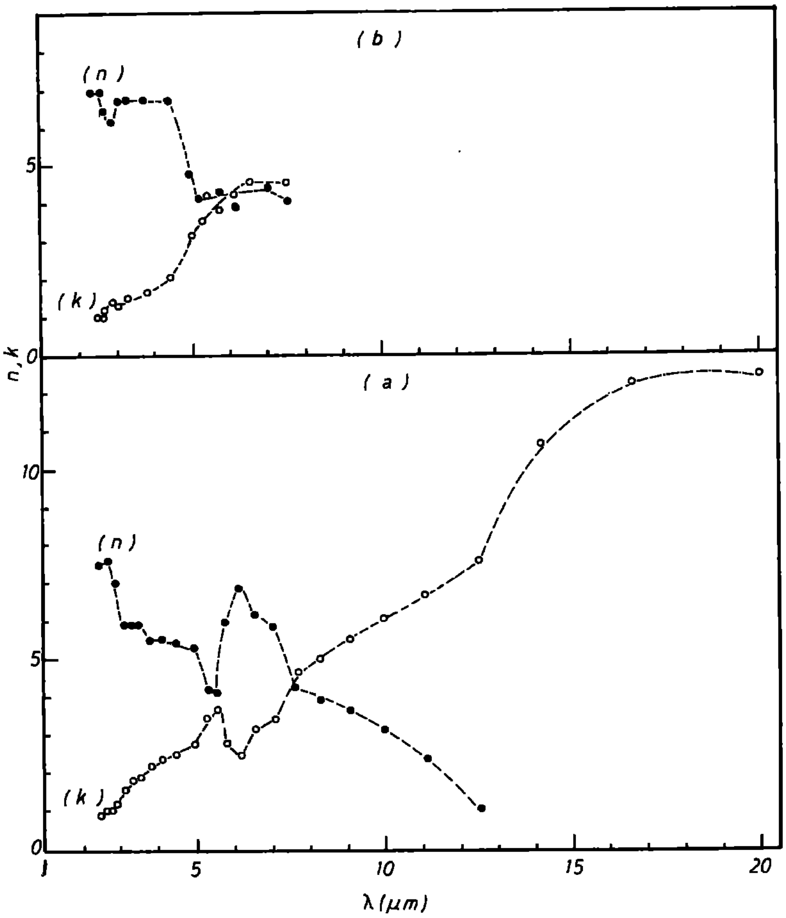

Figure 2 The dependence of the extinction coefficient (k) and refractive index (n) on wavelength: (a) $t = 150$ nm on KBr disc; (b) $t = 120$ nm on mica substrate.

$m = 9.1 \times 10^{-28}$ gm is the mass of the free electron, ω is the light frequency, ν_0 is the effective collision frequency of the conduction electrons and ω_0 is the plasma frequency. In terms of Drudés relation

$$\bar{\varepsilon} = \varepsilon + i\,\frac{4\pi\bar{\sigma}(\omega)}{\omega} = (n - ik)^2 \qquad (4)$$

one obtains,

$$\sigma_1(\omega) = \frac{\varepsilon_2\omega}{4\pi} = \frac{nk\omega}{2\pi} = \frac{Ne^2\nu_0}{m(\omega^2 + \nu_0^2)} \qquad (5)$$

When $\omega \to$ zero, $\sigma_1(\omega) \to \sigma_{\text{d.c.}}$, hence

$$\sigma_{\text{d.c.}} = \frac{Ne^2\tau}{m} \qquad (6)$$

where τ is the relaxation time and is equal to one half the time between two collisions. In the spectral region, $\omega_0^2 \gg \omega^2 \gg \nu_0^2$ one obtains

$$\begin{aligned} Re\,\varepsilon &= \varepsilon_0 - \frac{\omega_0^2}{\omega^2} \simeq \varepsilon_0 - \frac{4\pi Ne^2}{m\omega^2} \\ &= \varepsilon_0 - \frac{Ne^2\lambda^2}{\pi mc} \qquad (7) \end{aligned}$$

and the relation between $Re\varepsilon$ and λ^2 should be linear. Fig. 3 shows such a relation in the visible and infrared region. The data were fitted with a correlation coefficient of 98.8%, 98.3% and 96.5% for a fused silica substrate, KBr disc and mica substrate, respectively, using a mini-computer TI 59. If one considers $\omega \approx \nu_0$ Equation 7 can be written in the form

$$Re\,\varepsilon = \varepsilon_0 - \frac{Ne^2\lambda^2}{2\pi mc^2} \qquad (8)$$

The value of N determined from the slope of the linear plot from Equation 8 is given in Table I.

As $\lambda^2 = 0$ the intercept on the ordinate axis gives $\varepsilon_l = 4.2$, 33.04 and 54.6 for a fused silica substrate, KBr disc and mica substrate respectively. The value of ε_l, KBr disc, could be taken as a good agreement with the known theoretical value of bulk tin [20] which is equal to 23.8.

The value of the relaxation time τ was determined according to the Drude equations which may be rewritten as

$$n^2 - k^2 - \varepsilon_l = 2nk\omega\tau = \frac{Ne^2}{m\varepsilon_0}\frac{\tau^2}{1 + \omega^2\tau^2} \qquad (9)$$

TABLE I Comparison between the physical parameters in the two regions

	Visible region	Infrared region	
		KBr disc	Mica substrate
Density of conduction electrons ($10^{22}\,N\text{cm}^{-3}$)	2.55	1.68	2.1
Density of conduction electron (N/atom)	0.688	0.455	0.57
Fermi velocity, V_0 ($10^8\,\text{cm sec}^{-1}$)	1.06	0.92	0.989
Relaxation time, τ (sec)	15×10^{-16}	0.526×10^{-14}	0.398×10^{-14}
Area of Fermi surface A_{eff} (10^{17} electron cm^{-3})	1.04	0.788	0.914
Plasma frequency, ω_0 ($10^{15}\,\text{sec}^{-1}$)	4.38	1.272	1.106
Contribution of conduction electrons to the absorption A_{el}	14.8%	5.19%	6.14%

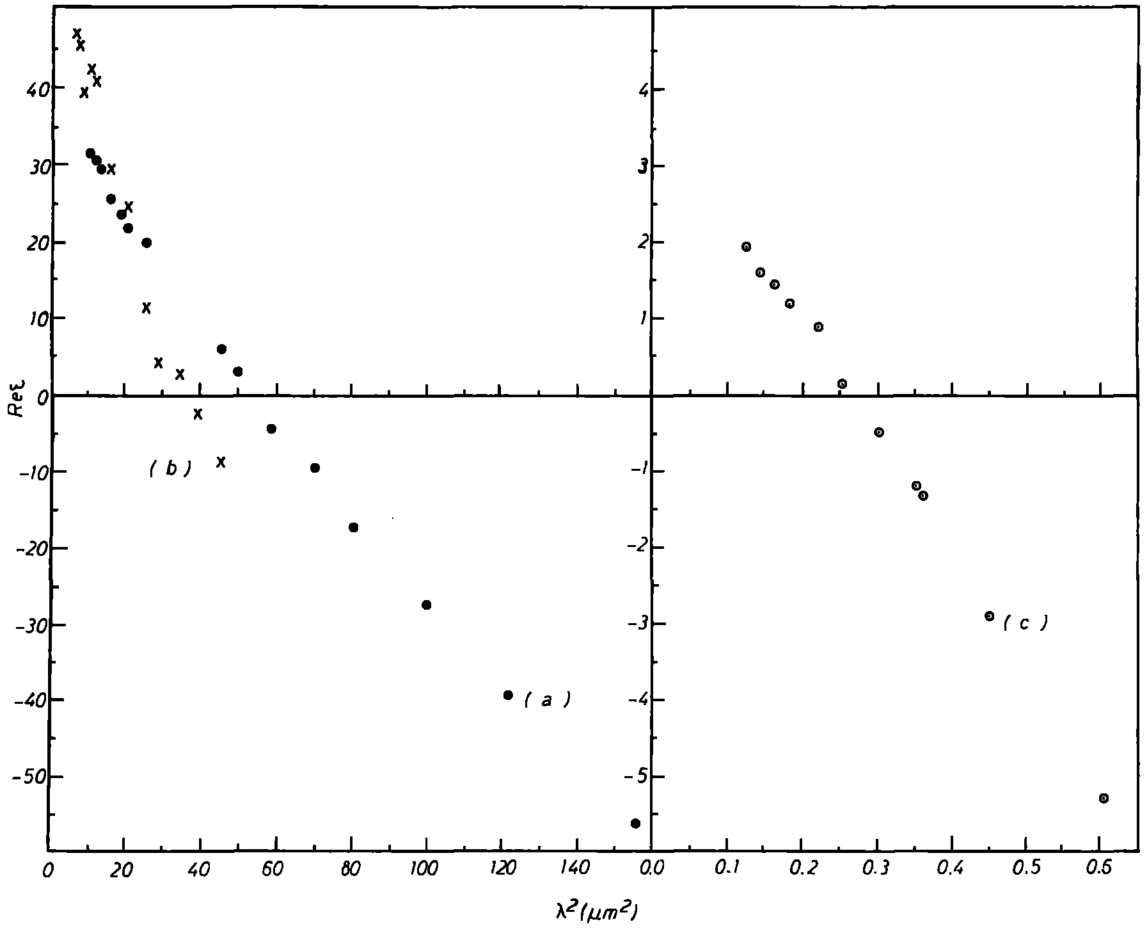

Figure 3 The dependence of the real dielectric constant $\varepsilon = n^2 - k^2$ on the wavelength (λ^2). (a) Tin deposited on KBr disc, (b) tin deposited on mica substrate, (c) tin deposited on fused silica.

Therefore, the value of the relaxation time τ was calculated to be 0.21×10^{-14} sec at $\lambda = 2.5\,\mu$m which is a reasonable agreement with the published theoretical values of tin [21] (0.23×10^{-14} sec).

By taking into account the fact that the measured d.c. conductivity [14] of the sample was $\sigma_{\text{d.c.}} = 2.24 \times 10^4\,\text{ohm}^{-1}\,\text{cm}^{-1}$ it can be calculated from Equation 6 that $v_0 = 1.899 \times 10^{14}\,\text{sec}^{-1}$. This value is smaller than the values estimated by Golovashkin and Motulevich [3, 4] and Macrae *et al.* [8] which are $2.26 \times 10^{14}\,\text{sec}^{-1}$ and $2.38 \times 10^{14}\,\text{sec}^{-1}$, respectively. On the other hand, the value of ω_0 was calculated as follows [22]

$$\omega_0 = \left(\frac{4\pi N e^2}{\varepsilon_1 m}\right)^{1/2} \tag{10}$$

and found to be $1.272 \times 10^{15}\,\text{sec}^{-1}$ which corresponds to $\lambda \sim 7.7\,\mu$m, that is, the short wavelength limit of the spectral region which is studied. Given the values of N and v_0 it is possible to evaluate the contribution of conduction electrons to the absorption A_{el}. By using the approximate expression [18]

$$A_{\text{el}} \approx v_0 \left(\frac{m}{\pi e^2 N}\right)^{1/2} \tag{11}$$

$A_{\text{el}} \approx 5.19\%$ is obtained. Thus the contribution of conduction electrons to the absorption in tin in the wavelength region of interest here is clearly very small. In the calculation presented above, it was assumed that skin-effect is normal in tin. Knowing the value of N, one can make the following evaluations. According to the equation [23]

$$V_0 = \left(\frac{h}{m}\right)\left(\frac{3N}{8\pi}\right)^{1/3} \tag{12}$$

the velocity on the Fermi surface is $V_0 \sim 0.921 \times 10^8\,\text{cm}\,\text{sec}^{-1}$ which agrees with the value obtained from the optical measurements of tin [3–5] ($V_0 = 0.93 \times 10^8\,\text{cm}\,\text{sec}^{-1}$), and the mean free path length [14] is $l \sim 0.0391\,\mu$m. The skin depth δ changes from 0.41 to $0.139\,\mu$m as the wavelength varies from 2.5 to $33.3\,\mu$m, as a result of which the condition for normal skin effect ($l \ll \delta$) is well satisfied over the whole region under investigation.

The values of the effective area of the Fermi-surface A_{eff} were determined in the case of the infrared and visible regions taking into account the following equation

$$A_{\text{eff}} = 4\pi(3\pi^2 N)^{2/3} \tag{13}$$

The results of the analysis of the experimental data are given in Table I.

It is clear from this table that there are great differences between these values. This discrepancy may be due to the skin anomalous effect which could obviously be found in case of the visible region rather than in the infrared, and also may be due to the evaporated tin films being deposited on different substrates which causes different granularities of the

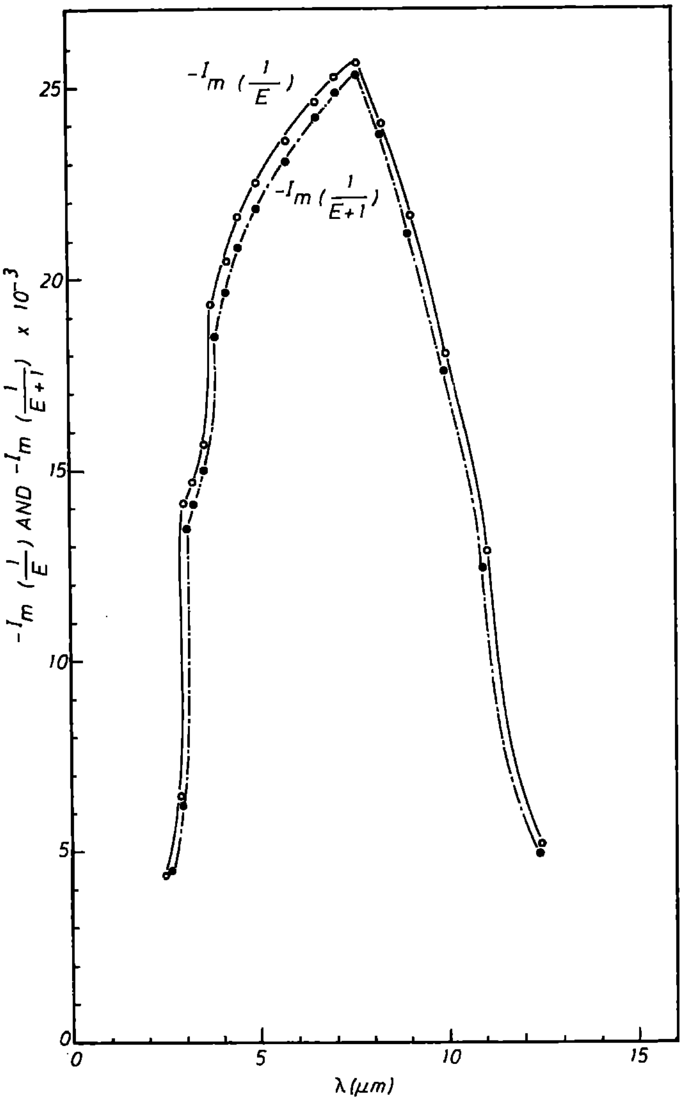

Figure 4 The behaviour of both the volume and surface energy loss functions as a function of wavelength. $t = 150$ nm tin deposited on KBr disc.

films. This phenomenon has been noted by other workers [13, 14]. In addition, it was found that the values of the relaxation time, τ, and the number of the conduction electrons N obtained from infrared measurements could be taken as reasonable values rather than those obtained from visible measurements. On the other hand, compared with the known value of Fermi velocity V_0 of bulk tin, it was found that V_0 obtained from the visible measurements was higher, while that obtained from infrared measurements was nearly the same. The high value of V_0 could be attributed to the fact that the photon energy $h\nu$ in the case of the visible region is larger than that in the case of the infrared.

The study of the anomalous skin effect showed that it is much greater in the case of the visible than in the case of the infared region. This is because the energy of the photon in the visible region is much higher than that in the infrared region leading to the movement of conduction electrons which would travel a considerable distance free from the applied electromagnetic field.

The volume $-I_m(1/E)$ and surface $-I_m[1/(E+1)]$ energy loss functions are proportional to the characteristic energy loss of fast electrons traversing the bulk and surface of the material, respectively. They are related to the real and imaginary parts of the dielectric constant by the relations

$$-I_m\left(\frac{1}{E}\right) = \frac{\varepsilon_2}{\varepsilon_1^2 + \varepsilon_2^2},$$

$$-I_m\left(\frac{1}{E+1}\right) = \frac{\varepsilon_2}{(\varepsilon_1 + 1)^2 + \varepsilon_2^2} \qquad (14)$$

where E is the complex dielectric constant.

Fig. 4 illustrates the behaviour of both the volume and surface energy loss functions. In Fig. 4 the $-I_m(1/E)$ and the $-I_m\,[1/(E+1)]$ function shows a sharp maximum at $\sim 7.7\,\mu$m. The sharpness of this maximum indicates that both energy losses should be observed when fast electrons traverse tin films.

Along with optical constants (n) and (k), the absorption coefficient A is of great importance in the description of a metal. The determination of the absorption coefficient [24] for normal incidence $A = 4n/(n+1)^2 + k^2$ indicated the presence of a sharp peak in the 3.1 to 3.8 μm region (Fig. 5).

References

1. P. BOUSQUET and P. ROUARD, *J. Phys. Radium* **21** (1960) 873.
2. G. RASIGNI and P. ROUARD, *J. Opt. Soc. Amer.* **53** (1963) 604.

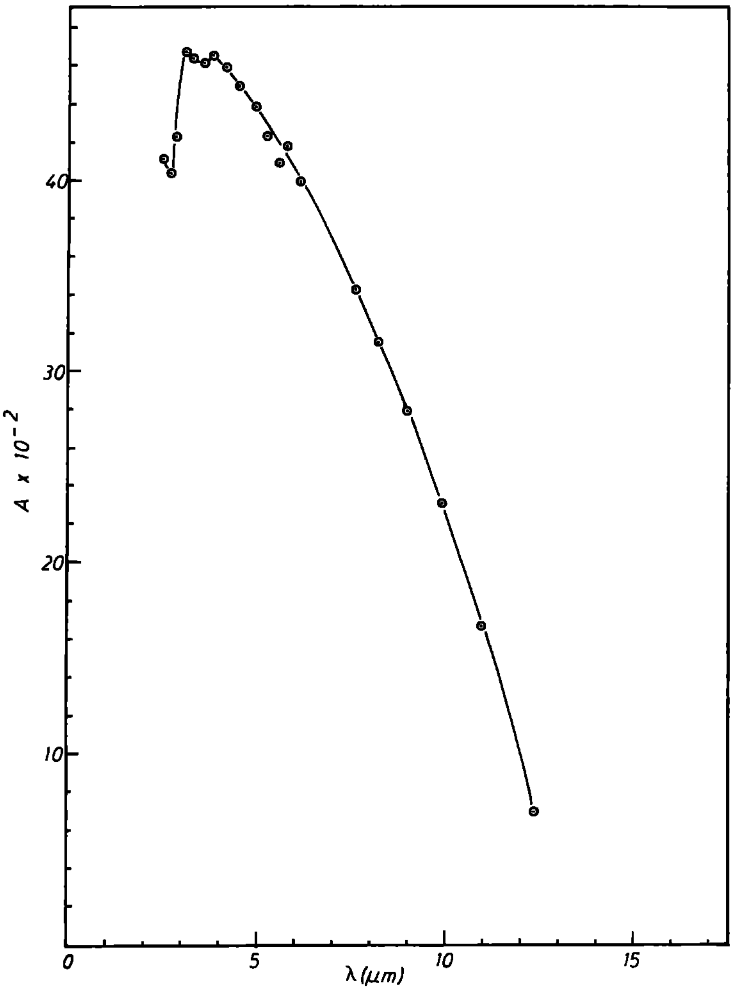

Figure 5 The variation of the coefficient of energy absorption with the wavelength. $t = 150$ nm tin deposited on KBr disc.

3. A. I. GOLOVASHKIN and G. P. MOTULEVICH, *Sov. Phys. JETP* **19** (1964) 310.
4. *Idem*, *ibid.* **46** (1964) 460.
5. *Idem*, *ibid.* **20** (1965) 44.
6. G. P. MOTULEVICH and A. A. SHUBIN, *Optika i Spectroskopiya* **2** (1957) 633.
7. J. N. HODGSON, *Proc. Phys. Soc. (London) B* **68** (1955) 593.
8. R. A. MACRAE, E. T. ARAKAWA and W. W. WILLIAMS, *Phys. Rev.* **162** (1967) 615.
9. N. R. COMINS, *Phil. Mag.* **25** (1972) 817.
10. C. M. HORWITZ, R. C. MCPHEDRAN and J. A. BEUNEN, *J. Opt. Soc. Amer.* **68** (1978) 1023.
11. E. A. ABOU-SAIF, A. A. MOHAMED and M. G. EL-KHODARY, *Thin Solid Films* **94** (1982) 133.
12. S. TOLANSKY, "Introduction to Interferometry" (Longman Green, London, 1955), p. 157.
13. K. D. CHOPRA, "Thin Film Phenomena" (McGraw-Hill, New York, 1969) p. 171.
14. Kh. A. MADY, S. MAHMOUD and A. H. EID, *Proc. Math. Phys. Soc. Egypt* **53** (1982) 9.
15. L. N. HADLEY and D. M. DENNISON, *J. Opt. Soc. Amer.* **37** (1947) 541.
16. L. HARRIS and A. L. LOEB, *ibid.* **45** (1955) 179.
17. L. G. SCHULZ, *ibid.* **43** (1953) 406.
18. V. L. JINZLURG and G. P. MOTULEVICH, *Uspekhi Fiz. Nauk.* **55** (1955) 469.
19. C. KITTLE, "Introduction to Solid State Physics" (Wiley, New York, 1971).
20. J. C. PHILLIPS, *Phys. Rev. Lett.* **20** (1968) 550.
21. N. W. ASHCROFT and N. DAVID MERMIN, "Solid State Physics" (Helt Rinehart and Winston, 1976).
22. YI-HAN KAO, *Phys. Lett.* **18** (1965) 16.
23. FREDERICK SEITZ, "The modern theory of solids" (McGraw-Hill, New York, 1940) Ch. IV.
24. L. N. SHKLIAREVSKI, A. A. AVDENKO and V. G. PADALKA, *Optics and Spect.* **6** (1959) 336.

Received 6 February
and accepted 6 May 1986